nuclear fusion
IAEA

PAPER

A study on hydrogen absorption and dissolution in liquid lithium

To cite this article: M. Christenson *et al* 2019 *Nucl. Fusion* **59** 026011

View the article online for updates and enhancements.

Recent citations

- Effect of N2 on release behavior of D2 in liquid lithium
L. Li *et al*

- Lithium, a path to make fusion energy affordable
A. de Castro *et al*

- A risk investment evaluation method based on dynamic bayesian network and fuzzy system
Xie Lechen *et al*

IOP ebooks™

Bringing together innovative digital publishing with leading authors from the global scientific community.

Start exploring the collection–download the first chapter of every title for free.

This content was downloaded from IP address 130.126.255.66 on 16/09/2021 at 21:05

IOP Publishing | International Atomic Energy Agency Nuclear Fusion

Nucl. Fusion **59** (2019) 026011 (11pp) https://doi.org/10.1088/1741-4326/aaf587

A study on hydrogen absorption and dissolution in liquid lithium

M. Christenson[a], D. Panici, C. Moynihan, J. Wendeborn, J. Anderson and D.N. Ruzic

Department of Nuclear Plasma and Radiological Engineering, University of Illinois at Urbana-Champaign, Urbana, IL 61801, United States of America

E-mail: mpchris23@gmail.com

Received 3 May 2018, revised 19 November 2018
Accepted for publication 3 December 2018
Published 4 January 2019

Abstract

Methods that plan to recover tritium from liquid lithium require intimate knowledge of the surface, sub-surface, and bulk chemistry associated with the interactions between hydrogen isotopes and lithium particles. Focusing on the lithium–lithium hydride system, previous studies have been able to determine concentrations associated with the liquidus curve, which separates the hydrogen dissolved in solution (known as the α phase) from the hydrogen which precipitates out as lithium hydride (known as the β phase). Knowledge of how these phases coexist in bulk melts is particularly important when the lithium is exposed to a hydrogen, deuterium, or tritium plasma, because they govern how quickly one can recover these isotopes in back-end processes for future lithium-walled fusion reactors. To this end, lithium samples were exposed to hydrogen plasmas in the Tungsten Fuzz Characterization of Nanofeatures (TUFCON) chamber at the University of Illinois. Each lithium sample was varied with respect to sample temperature, applied electrical bias, and length of sample exposure, and in each there coexisted a combination of the α and β phases. In all cases, two distinct absorption periods were observed during exposure. Similarly, two distinct desorption periods were observed during temperature-programmed desorption (TPD) scans. While similar desorption periods have been observed in the literature, changes in sample resistivity measured in the current study help to validate this behavior from a novel, condensed-phase perspective. The results of lithium exposures in TUFCON will be presented, along with a discussion on how the exposure conditions and phases affect recovery. Observations of superficial surface layers, and how they affect absorption and desorption, will be included in these discussions. How these results, along with the resultant marginally-enhanced dissolution behavior, can extend to tritium recycling efforts will also be explored.

Keywords: plasma-facing component, liquid lithium, hydrogen isotope, absorption, dissolution, desorption, phase separation

(Some figures may appear in colour only in the online journal)

1. Introduction

Recently, lithium (Li) has gained interest as a possible fusion first wall material due to its ability to enhance confinement [1] and consume impurities and cold fuel particles [2]. Despite many advantages, skeptics to the in-vessel application of lithium are concerned with its ability to retain fuel species, specifically tritium (T). This is because of the radiation concerns surrounding tritium use, as well as the fact that there is very limited isotope availability. Focus must therefore be shifted to tritium recovery efforts in order for lithium to be more widely considered. These back-end recycling technologies require intimate knowledge of the surface, sub-surface, and bulk chemistry associated with the interactions between the captured tritium and lithium.

Early work done by Veleckis *et al* [3–6], Adams *et al* [7], and others [8, 9] investigated how chemical phases were separated in solution for lithium–lithium hydride and

[a] Author to whom any correspondence should be addressed.

 © 2019 IAEA, Vienna Printed in the UK

lithium–lithium deuteride systems. Focusing on the lithium–lithium hydride system, they were able to determine concentrations associated with the liquidus curve, which separates the hydrogen dissolved in solution (known as the α phase) from the hydrogen which precipitates out as lithium hydride (known as the β phase). In his studies, Baldwin *et al* [10, 11] was able to observe how the deuterium present in these separate chemical phases affected his temperature-programmed desorption (TPD) results. Baldwin claimed that at temperatures below the melting temperature of the hydride or deuteride salt, the initial hydrogen release (desorption period 1) was due to the evolution of hydrogen from the α phase, and the following release of hydrogen (desorption period 2), at temperatures near the melting point, was due to dissolution of, and subsequent evolution from, the β phase. Similar observations for desorption behavior have been reported in several other studies [6, 9, 10, 12, 13], all of which identified two distinct evolution rates. Identification of these desorption periods is vital for back-end tritium recovery efforts.

Many studies [14–20] have found that the presence of a plasma enhances the solubility of diatomic gases well above the limits predicted by Sieverts law [20]. Mundra's group [14] defined a more universal model for the solubility of diatomic gases in liquid metals, arguing that enhanced solvation was due to interactions of charge carriers at the surface. Through inelastic collisions at the surface, ions regain electrons to become energetic neutrals. Mundra proposed that these species, specifically the monatomic species, are what create a state of 'supersaturation' within the liquid metal [14]. Mundra did go on to state that a limit to this theory exists if a new species is formed (e.g. lithium hydride, lithium deuteride, or lithium tritide); however, if Mundra's hypothesis is true or not for the lithium–lithium hydride system remains unclear.

Another factor that affects hydrogen absorption and desorption is the presence of a surface layer, which grows in the absence of agitation. Earlier studies performed by Veleckis [3, 4] and others [8, 9], which used pressure decay to define the liquidus curve, attributed deviations in their predicted absorption values to the formation of similar surface layers. Whether they be from the presence of impurities or the formation of solid LiH 'crusts', these surface layers impede absorption, especially when the sample is maintained below the monotectic temperature (i.e. the LiH melting point). Desorption behavior is affected similarly, such that excess energy is required to disperse the established surface layer, on top of that which is needed to evolve hydrogen. Details on this layer's dependence on plasma exposure conditions will be discussed in this report, along with how they may impact recycling efforts.

To this end, lithium samples were exposed to hydrogen plasmas in the Tungsten Fuzz Characterization of Nanofeatures (TUFCON) chamber at the Center for Plasma-Material Interactions [21]. The TUFCON chamber was used because out of all low-temperature plasma sources, helicons can most closely mimic magnetic confinement conditions in larger toroidal devices. TUFCON was outfitted with a residual gas analyzer (RGA) for TPD analyses, optical emission spectroscopy (OES) system for real-time retention analyses, and a custom-fabricated resistivity probe for condensed phase analyses. Lithium samples were varied with respect to sample bias, sample temperature, and length of sample exposure to investigate how all of these variables affected retention and desorption. The goal of this study was to characterize how the α and β phases contribute to the hydrogen absorption and desorption properties in liquid lithium, and how hydrogen is distributed into these different phases.

This paper presents the work accomplished at the Center for Plasma-Material Interactions to investigate how plasmas contribute to the hydrogen-lithium chemistry. The results demonstrate evidence of two distinct absorption and two distinct desorption periods, as well as evidence of an insulating surface hydride layer, both of which have important implications for tritium recovery. While two distinct desorption periods for this system have been previously observed, it will be shown that changes in resistivity can more strongly link such periods to the different phases present within the sample, from a novel, condensed-phase perspective.

Section 2 describes the TUFCON chamber and diagnostics with which retention and desorption measurements were made. This includes how each sample was procedurally exposed to a hydrogen plasma, and subsequently characterized during TPD. Section 3 presents the results from these experiments, while describing how temperature, bias, and time modified the outcome. Section 4 discusses the impact of these results both from a fundamental point-of-view, as well as from the perspective of tritium recovery in larger liquid lithium loops. Finally, section 5 summarizes the results and describes future experimental work.

2. Experimental setup

2.1. TUFCON chamber

The chamber used in this work was a modified version of the TUFCON experiment [21]. This chamber was chosen because its helicon plasma was driven by a MORI 200 source [22, 23], meaning the hydrogen plasma would have a relatively high density, while having its ions confined along field lines. Although this helicon plasma is not entirely representative of a reactor-scale plasma, it is a more accurate representation of the reactor environment than an ion beam because exposure to a helicon plasma takes into account the effect of electrons and sheath kinetics on plasma-surface interactions [24]. A block schematic of the TUFCON chamber, together with the added TPD antechamber, can be seen in figure 1.

In order to accurately ascertain the amount of hydrogen being absorbed and released in a sample, a calibration between hydrogen flow rate and the partial pressure read by the RGA was performed. Hydrogen flow rate was controlled by an AliCat mass flow controller and compared to the MKS Baratron pressure and RGA partial pressure response of mass = 2 AMU. The location of the hydrogen inlet was the same as the sample location during TPD. This calibration, along with the appropriate equation of state, was used to find the particle evolution rate from the sample surface. To account for the residual hydrogen in the chamber, minimum partial pressures observed during the trend scan were subtracted from the trend

scan as a whole. These residual pressures were often found to be 2 or more orders of magnitude lower than typical trend scan pressures [24].

Plasma conditions were analyzed using an RF compensated Langmuir probe and an uncompensated Langmuir probe. The probe actively sampling the plasma was the RF compensated probe, oriented with the probe tip facing up and positioned where the sample would be during exposure. The second, uncompensated probe was held in roughly the same position and orientation as the RF compensated probe, but set radially apart by approximately 3.8 cm. This second probe was used to investigate the floating potential in the plasma. Figure 2 [24] depicts a representative I–V trace at 30 mTorr and a helicon power of 500 W. Note that all hydrogen pressures have been corrected by gas calibration.

For the pressure and the RF power used during exposures (30 mTorr and 500 W), the electron temperature was found to be 5.2 ± 1.0 eV, while the electron density was found to be $(3.3 \pm 0.7) \times 10^{18}$ m^{-3} [24], at a floating potential of approximately 25 V. This equates out to an instantaneous, unbiased ion flux of $(1.1 \pm 0.1) \times 10^{22}$ m^{-2} s^{-1}, which will be used in all future flux and fluence calculations [24] and assumed constant over the lithium surface. A -50 V bias modifies the flux to $(7.2 \pm 1.5) \times 10^{22}$ m^{-2} s^{-1}, while a -100 V bias modifies the flux to $(1.0 \pm 0.2) \times 10^{23}$ m^{-2} s^{-1}, based on the theoretical ion matrix sheath dependence on sample bias [24].

2.2. Diagnostics

A battery of diagnostics were employed in the TUFCON chamber to investigate the hydrogen absorption and desorption properties in lithium, and how the chemistry affects these properties when lithium is exposed to a plasma. Apart from the Langmuir probes used to define the plasma conditions, this included an RGA for TPD analyses, optical emission spectroscopy (OES) for real-time retention analyses, and a custom-fabricated resistivity probe for condensed phase analyses. The resistivity probe was a particularly enabling technology, as it was able to help confirm the presence of two desorption periods as registered during TPD, which were also previously witnessed in Baldwin's studies [10, 11].

A Mikropack PlasCalc-2000-UV/VIS/NIR spectrometer was used for the OES scans, which can measure signals between 190 and 1077 nm in wavelength. These OES scans were used to qualitatively observe absorption behavior. The OES analysis provided spectral intensity sampled over the duration of the plasma exposure, which could be examined relative to initial line intensities measured before plasma breakdown. Background intensities have been accounted for in the signals reported herein. Spectral emission for H_α, H_β, Li_I, and Li_{II} transitions were observed at wavelengths of 656.3, 486.1, 550.3, and 671.1 nm respectively. A representative plot of the spectral emission for H_α can be seen in figure 4. Li lines were monitored to investigate emission trends with respect to exposure conditions. The expectation was that Li intensities would rise and fall inversely to the trends observed for the H_α and H_β lines due to the initial sputtering and excitation of lithium near the sample surface. This was true in all experiments. It should be made clear that the OES measurements are only meant for illustrative and qualitative purposes, and serve primarily to identify hydrogen absorption behavior. Any further analysis from these OES measurements, specifically the H_β and Li measurements, will be left to future work.

A Vacuum Technologies, Inc. AeroVac Odyssey 150 mass spectrometer was used to monitor the partial pressures for masses of 1, 2, 6, 7, 18, and 28 AMU. Of specific interest were those signals pertaining to 1 and 2 AMU, which represented atomic and molecular hydrogen, respectively. Two desorption periods were observed, similar to those described

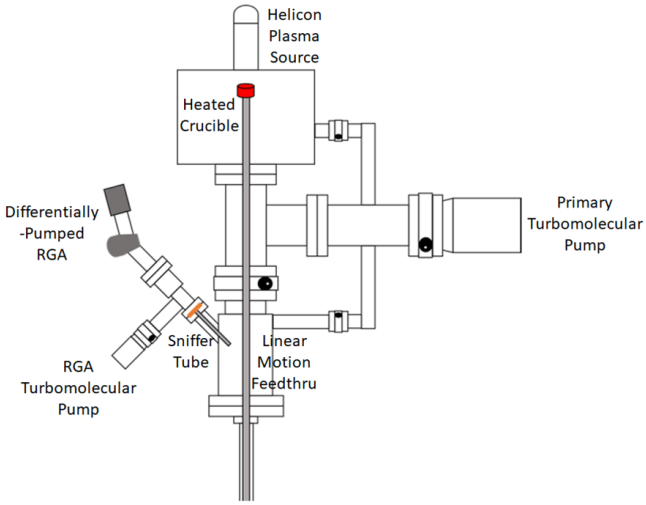

Figure 1. A block schematic of the TUFCON chamber used for exposing lithium samples to hydrogen plasmas under various conditions [24]. In this image, the sample crucible is in its position for plasma exposure. During TPD, the sample is retracted down to the antechamber, where partial pressures of gases desorbing from the lithium are registered by the RGA. Reproduced with permission from [24].

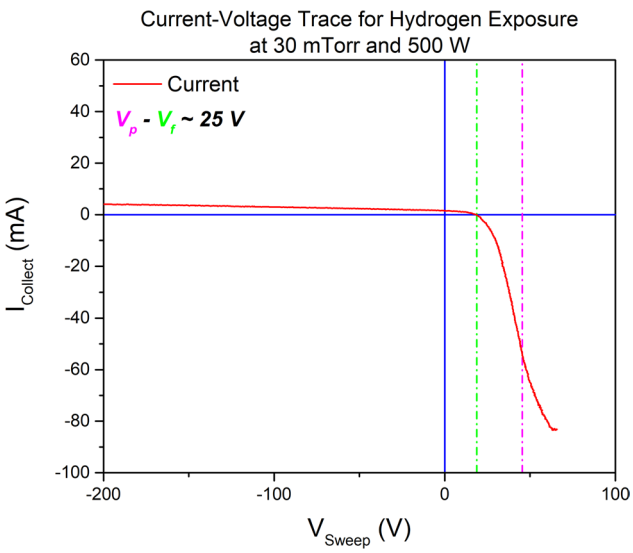

Figure 2. A plot of the current–voltage characteristic from an RF-compensated Langmuir probe for a TUFCON hydrogen plasma at 30 mTorr and 500 W. The resistor used for the current measurement in this case was 2.181 kΩ [24]. Reproduced with permission from [24].

by Baldwin [10, 11], which was also confirmed by resistivity changes observed during TPD. The resistivity in the sample was measured between two concentric, cylindrical steel electrodes. These measurements and their implication will be discussed in more detail in section 3.

2.3. Exposure procedure

The lithium exposure and measurement procedure in TUFCON is outlined in the block diagrams in figure 3. Great care was taken to ensure the highest possible purity of lithium sample, with the loading, transport, and insertion of the crucible all being done under actively-purged argon atmospheres. Transport from an argon-purged drybox was carried out in an argon-filled bag, where it was transferred to the heater test stand situated in the process chamber. The chamber was also actively purged with argon during transfer. This procedure was chosen to maximize sample integrity during loading and pumpdown. With hydrogen fill, reactive gas partial pressures in the chamber post-pumpdown were found to be four to five orders of magnitude less than the species of interest. Quantitatively, the H_2O signal was measured on the order of 1×10^{-9} Torr, whereas the H_2 signal was measured between 1×10^{-6} to 1×10^{-4} Torr. Without hydrogen fill, absolute partial pressure values were lower, but impurities were a higher percentage of the overall gas composition. By the time the exposure began, a few monolayers of impurity on the Li may have formed. As will be described later, pre-exposure bakes (at temperatures higher than the exposure temperatures) were employed to prevent Li reactivity and liberate surface impurities. Even when the sample was heated, the impurity signals registered by the RGA were always orders of magnitude less than the species of interest. Similar procedures were performed by Baldwin during his exposures [10, 11].

The amount of lithium loaded for each trial was on the order of 0.20 ± 0.06 g, meaning that the number of Li atoms in the sample was on the order of $(3.3 \pm 0.9) \times 10^{22}$. The error associated with this measurement is the characteristic mass uncertainty for the sample. The crucible into which the sample was loaded was outfitted with an inner electrode and an outer electrode, in order to measure the resistance through the lithium sample.

The sample was then exposed to either hydrogen gas or plasma, following the procedure outlined in figure 3. Post-exposure, a Keithley 2000 Multimeter continuously measured the sample resistance. After the sample was transferred to the TPD antechamber and the remaining hydrogen was allowed to evacuate the system, the RGA was then absolutely calibrated to the base pressure measured by a Pfeiffer full-range gauge attached to the same differentially-pumped section. The RGA trend scan was then started, and the sample was heated from its starting temperature (the temperature maintained during hydrogen exposure) until the multimeter read that the sample resistance had elevated to the kΩ range from an initial resistance of tens of $\mu\Omega$s. While this drastic change in resistance will be explained in more detail later, it was indicative of a change in the sample chemistry during desorption. These results

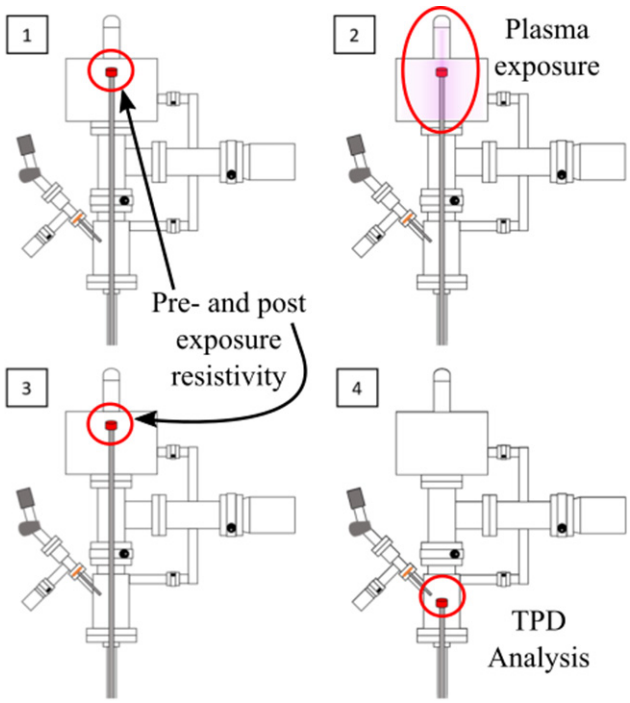

Figure 3. A block schematic illustrating the Li exposure and measurement procedure in TUFCON, annotated with the major steps occurring in each panel. OES signals were monitored during plasma exposure, and TPD scans were taken once the sample was withdrawn into the antechamber. Resistivity was also monitored during TPD. The sample was then heated until the multimeter read that the sample resistance had risen to the kΩ range. Reproduced with permission from [24].

were able to help confirm the presence of two desorption periods, as claimed by Baldwin [10, 11] and others [12, 13]. After each run, the crucible was cleaned by soaking in water and acetic acid multiple times to remove the lithium and lithium hydride respectively. When all of the lithium was removed, the crucible was cleaned with isopropyl alcohol and baked at 200 °C for 2 h to remove any residual water.

3. Results

3.1. Sample bias and exposure time dependences

How the applied electrical bias and duration of exposure affected the absorption and desorption properties will be described first. The three biases tested were such that the sample was left as a floating object, biased to −50 V, and biased to −100 V. These voltages correspond to ion doses of $(1.9 \pm 0.2) \times 10^{21}$, $(1.2 \pm 0.3) \times 10^{22}$, and $(1.7 \pm 0.4) \times 10^{22}$ hydrogen ions, respectively, each over an exposure time of (15 min ± 70 s). All doses in the varied bias experiments were below the saturation threshold (where $N_H = N_{Li}$). In this regime, there should exist both dissolved hydrogen and hydride precipitate within the solution [24]. For each experiment, the hydrogen pressure was held at 30 mTorr, and the RF power was held at 500 W. The hydrogen pressure was held constant through careful manipulation of the flow rate. The lithium samples were heated to temperatures in excess of 375 °C

and held for 15–20 min before cooling them down to the exposure temperature of 350 °C, which remained the same (within error of ±12.0 °C) between these experiments.

The three samples in the varied exposure time experiments were all exposed to the same plasma conditions (30 mTorr, 500 W, −50 V) for (15 min ± 70 s), (60 min ± 70 s), and (90 min ± 5 min). The latter two of these exposure times equate to doses that exceed the amount of lithium in a given sample, meaning that the 60 min and 90 min lithium sample exposures should have completely converted to hydride, assuming no hydride recycling occurred, as well as assuming no insulating surface hydride layer had formed to inhibit absorption. From the pre- and post-exposure resistivity measurements, the dramatic rise associated with a total conversion to lithium hydride was not observed.

Observing the spectral emission, the degree of absorption can be broken down into what appears to be two distinct periods. This is shown in figure 4 [24], where a representative OES scan, tracking the H_α signal, for a sample held at 250 °C is displayed. The values in the figure are for illustrative purposes. The 62% drop highlights the magnitude with which the emission spectrum changes in the first absorption period, while the 6.8 min identifier depicts the relative time in which the sample remains in this first absorption period.

The H_α OES responses as a function of time for various sample biases and exposure durations are shown in figure 5 [24]. From the OES responses with respect to sample bias, it is seen that as a more negative sample bias is applied, the amount of time spent in the first absorption period increases significantly. As the bias becomes more negative, the ions impacting the sample increase in energy, so their range into the lithium likewise increases. This means that a higher hydrogen population is necessary to create a surface layer, which will be made thicker in samples with a more negative bias. This is why the −100 V biased sample appears to spend more time in the first absorption period. The H_α OES responses with respect to exposure duration show a gradual decrease in the H_α signal over time. This is likely due to the diffusion of the insulating superficial hydride layer away from the surface. This process exposes more lithium which more readily absorbs hydrogen, replenishing the hydrogen lost by the diffusion into the bulk and increasing the overall amount of hydrogen in the bulk. Higher ion bombardment energies may also result in the breaking up or mixing of the inhibiting layer, which could also help in revealing a fresh top layer which can more readily absorb. The combination of hydrogen diffusion into the bulk, or the mixing of the superficial surface layer, and replenishment at the surface is considered to be the mechanism with which a non-agitated lithium sample will be entirely converted to hydride. While future work should be done to validate this claim, its implication is an important step in understanding the chemistry and kinetics for the Li–H system.

Post-exposure, sample chemistry was then characterized by investigating trends in the desorption properties. Resistivity was used to monitor the degree of desorption and evaporation during the TPD portion of each experiment. Figure 6 [24] depicts a result representative of each sample exposed to a plasma in TUFCON. The resistivity results represented

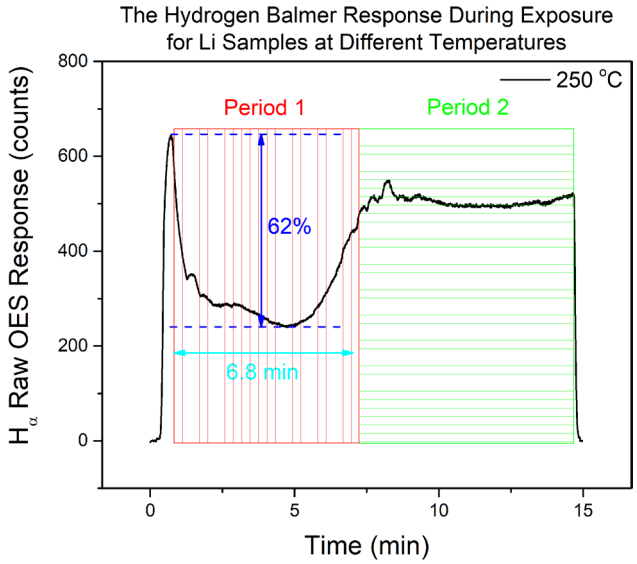

Figure 4. A representative H_α trend for the sample exposed at 250 °C to 30 mTorr of hydrogen at an RF antenna power of 500 W. The second absorption period was identified as the point where the H_α intensity began to level off at higher values. Reproduced with permission from [24].

in figure 6 are very important, because they help to support Baldwin's conclusions [10, 11] that contributions to hydrogen release are dominated by the different phases during different desorption periods. Contributions to the first period derive primarily from the α phase, where lower resistivity measurements across the sample are still observed (similar to those that would be observed through a conducting lithium pathway). Once this source has been depleted and the free lithium has evaporated, which accompanies the release of hydrogen from the α phase, the β phase becomes the sole source of hydrogen, which is indicated by higher resistivity measurements across the sample during the plateau period. Separating these two contributions based on resistivity, one can determine how much hydrogen was initially allocated to each phase to see if plasmas do enhance dissolution properties in the hydrogen-lithium system. This is a very important result, and will be presented in more detail in section 4.

The influence from each of the species of interest can be used to qualitatively explain the trends in figure 6. After exposure, hydrogen in the sample exists simultaneously in the α and β phases. Free lithium is also present since hydrogen in the α phase is not strongly bonded to its neighbors. This free lithium is what establishes the conducting pathway between the concentric electrodes of the resistivity probe. As temperature is increased, hydrogen evolves from the α phase and escapes as gas. Lithium is left behind, now with less and less dissolved hydrogen to act as impurities for electrical scattering, which is why during 'Period 1' the measured resistivity gradually decreases. When comparing this result to Adams' work [7], this gradual downward trend makes intuitive sense—less dissolved hydrogen results in a more conductive sample. At the end of 'Period 1', the remaining free lithium fully evaporates from the sample, which is also evident in the temperature versus time subplot. The slight dip observed in temperature, after an hour into the experiment,

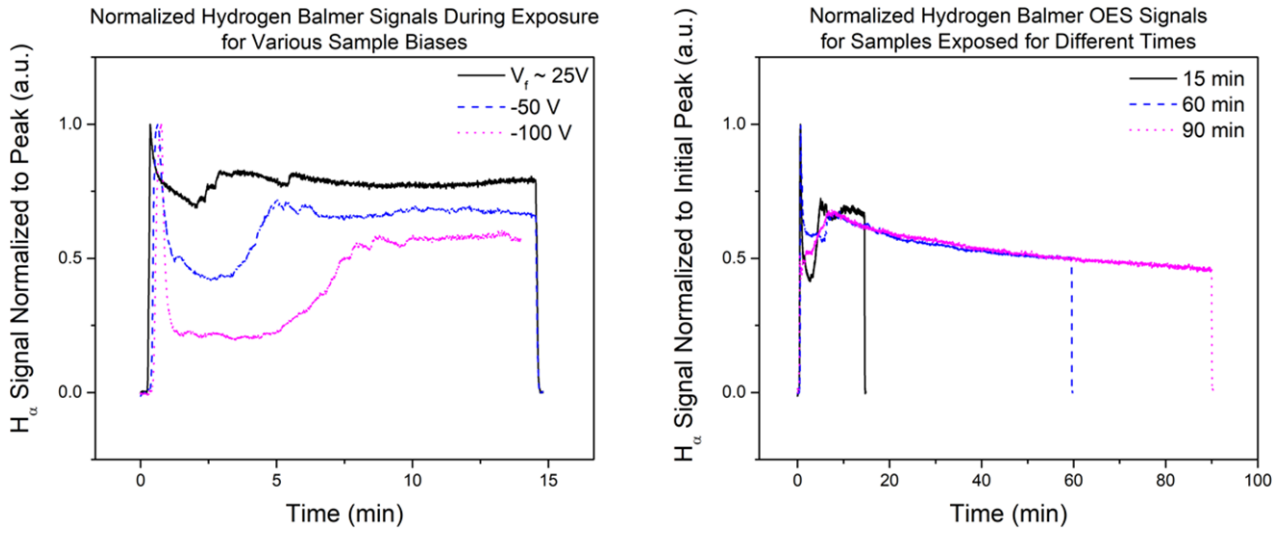

Figure 5. The H_α OES responses, normalized to the peak intensities in Period 2 absorption, as functions of time for (left) samples subjected to different levels of external biasing, and (right) samples exposed for different periods of time. Reproduced with permission from [24].

is assumed to be due to the fact that much of the heat being applied is consumed as lithium changes phases (where the bulk of the remianing, free liquid lithium is evaporating). A portion of this heat is also being consumed to dissolve the β phase LiH salt, in order to maintain a pseudo-equilibrium state. Once the remaining free lithium is evaporated, the resistivity begins to rise exponentially, as the only remaining path between electrodes is through the now-dissolving LiH salt. Once the plateaus in 'Period 2' are reached in both pressure and resistivity, the remaining sample is LiH, which acts as the sole source of hydrogen and the only 'conducting' path. The sample will then continue to progress in this state, with β phase dissolving to α phase where both the free hydrogen and lithium are immediately released, until the entire sample volume has been depleted.

The formation of thicker surface hydride layers, and hydride diffusion into the bulk at longer exposure durations, also affects desorption. Under the assumption that the first desorption period is dominated by evolution from the α phase, the peak release fluxes associated with this phase were evaluated. These fluxes are indicative of what one could expect in solutions where the hydrogen isotope concentration is below the solubility limits. Peak release fluxes registered during TPD scans and the associated variable (bias or exposure duration) for these experiments are shown in figure 7 [24]. As can be seen in the plot on the left, a more negative bias results in a reduced peak release flux. Any surface hydride layer established is likely to be thicker, and more energy is needed to disperse this thicker layer so that α-phase hydrogen can be released. Thus, smaller fluxes result from the sample. From the plot on the right, it can be seen that longer exposure times resulted in elevated release fluxes, meaning that there was a greater population of hydrogen in the bulk, which would have been proportionally distributed into the α and β phases. This makes sense, considering that the hydride diffusion process, described in the following section, would allow more hydrogen to dissolve into the bulk the longer the sample was exposed.

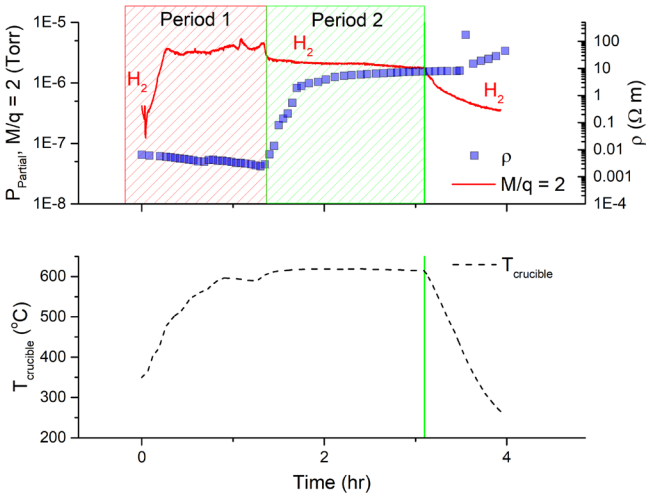

Figure 6. Data for the raw 2 AMU RGA signal and the resistivity measurement taken during the TPD portion of the experiment for the sample exposed at 350 °C. There are two desorption periods, which are dominated by contributions from hydrogen in the α phase in the first period and from the β phase for the second period. It was found that had TPD scans continued to the point where all H_2 was released, then an individual experiment would have lasted more than 10 h. Vacuum hardware limited such lengthy tests. Reproduced with permission from [24].

3.2. Temperature dependence

The temperature dependence on absorption and desorption behavior in this study both verified past works and also offered new insights into the dynamics of the surface layer. Sample temperature has an impact on whether LiH precipitate forms (β phase) or hydrogen dissolves into the melt (α phase) upon absorption of a hydrogen ion, radical, or neutral. In this case, radicals refer to species energized beyond their ground state valency, typically having an unpaired electron. This makes radicals highly chemically reactive.

In all experiments listed in this section, the only variable modified was the sample temperature during exposure. For each experiment, the exposure time was set to 15 min, while

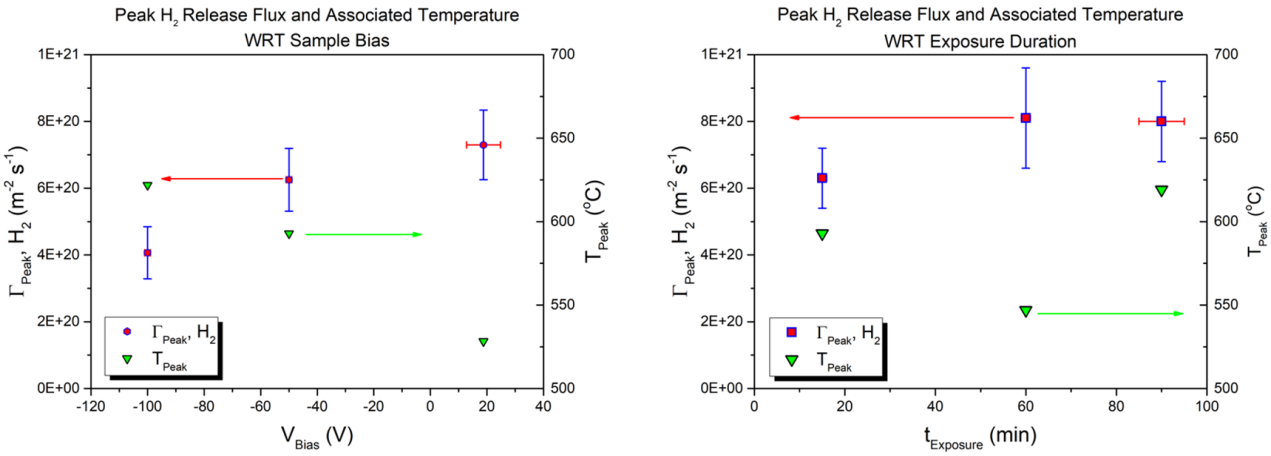

Figure 7. The peak release fluxes and the associated temperatures as a function of (left) the sample bias during exposure and (right) the duration of exposure. Reproduced with permission from [24].

the pressure and RF power remained the same as in the previous section. Each sample was biased to −50 V, meaning that the total plasma fluence to the sample over 15 min was approximately $(6.5 \pm 1.4) \times 10^{25}$ m^{-2}. This equates to doses of approximately 38% of the saturation threshold, so hydrogen should exist in both phases simultaneously.

From the spectral emission of the H_α and H_β signals, the durations and relative intensity changes for the different absorption periods are shown in figure 8 [24]. While the aim was to expose the samples at different temperatures for a total of 15 min, some discrepancy existed with regards to the total exposure duration, as shown in figure 8. This variability affected, to a minor degree, the recovery measurements. As will also be explained later, the separation of the two absorption periods is affected by the establishment of a superficial surface layer.

From solely the spectral responses, it appears the absorption periods are broken up such that the lower temperature samples spend more time in the first absorption period than do the higher temperature samples. Again, it should be noted that the spectral responses were only used as a qualitative observation. The information used from these observations were the approximate times each sample spent in each absorption period. The times spent in the first absorption period account for $45 \pm 9\%$, $60 \pm 12\%$, $26 \pm 6\%$, and $28 \pm 6\%$ of the total exposure time for each sample, respectively. The total ion dose to the sample was approximated by assuming a constant flux to the sample during exposure, converting that to fluence and normalizing by sample surface area. Total exposure durations are based on the summation of the times for a given sample in figure 8.

What is likely happening is that at higher sample temperatures, the energy barrier to form hydride is reduced, a trend which has been previously reported [25]. This means that any surface insulating layer will be established faster in liquid samples at higher temperatures. The differences in the Period 2 absorption shown in figure 8 [24] are then due to the diffusion of hydrogen away from the surface, which is also enhanced with temperature. It is worth mentioning that such surface layers were visually observed post-mortem and were not seen in trials without hydrogen plasma exposure. As was mentioned in the Introduction, earlier works [3, 4, 8, 9] also described the effects of similar surface layers. Figure 8 [24] deals with the changes in H_α signal relative to the initial plasma condition for each absorption period, with higher sample temperatures leading to smaller differences in intensity between the two absorption periods.

The peak values for hydrogen release flux observed during TPD, along with the associated temperatures for this experiment set, are shown in figure 9 [24]. This plot is similar to figure 7, but the data is with respect to sample temperature. Overall, the maximum evolution flux is $(7.6 \pm 1.1) \times 10^{20}$ H_2 particles m^{-2} s^{-1}. More detail on what these values mean for recovery efforts will be presented in section 4.

4. Discussion

Results from the exposure of lithium samples to hydrogen plasmas under different conditions were reported in the previous section. This section will be used to discuss what these results mean with regards to absorption and desorption properties, and how this affects tritium recovery efforts as a whole. First, focusing on the effects that sample temperature has on the hydrogen-lithium chemistry, one of the more interesting results to come from the work done in TUFCON is shown in figure 10 [24]. Using the point where the resistance drastically changes during TPD, as seen in figure 6, as an upper bound, one can determine the amount of hydrogen that was initially dissolved into the lithium by integrating the instantaneous hydrogen evolution rates (H_2 molecules per second) over time up to this upper bound. In looking at how sample temperature affected the lithium-hydrogen chemistry, these results were then compared to theory [26] used to define the liquidus curve in the lithium–lithium hydride phase diagram. From the plots in figure 10, experimental dissolution trends approach thermodynamic predictions at higher exposure temperatures, but deviate significantly at lower exposure temperatures. While this may be due to the fact that at lower temperatures the additional kinetic energy provided by the plasma plays a more pivotal role in the hydrogen absorption chemistry, further

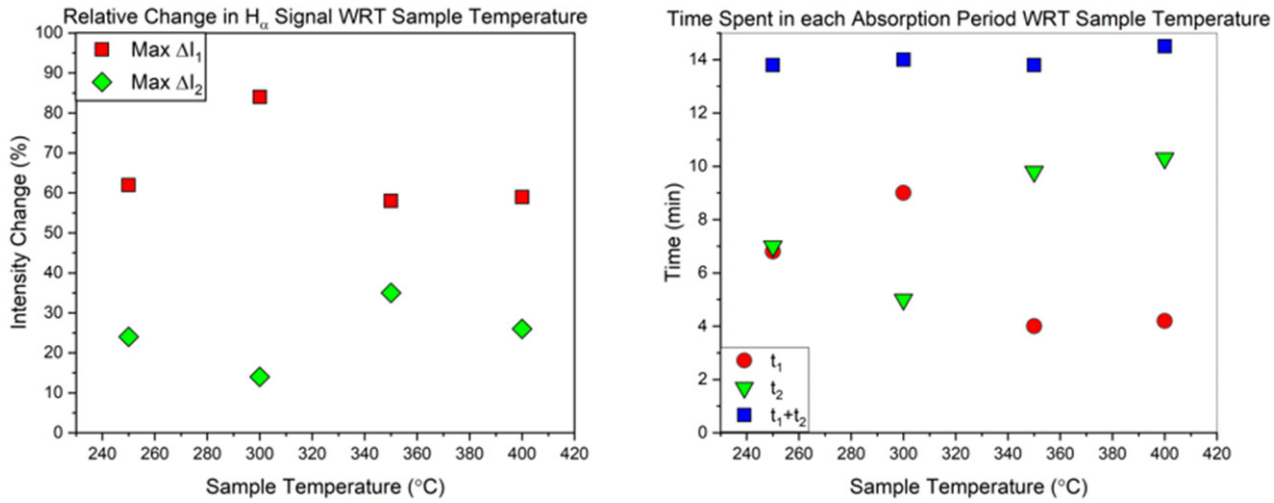

Figure 8. The times spent in each absorption period (right) and the associated maximum change in H_α relative intensity (left) with respect to temperature. Reproduced with permission from [24].

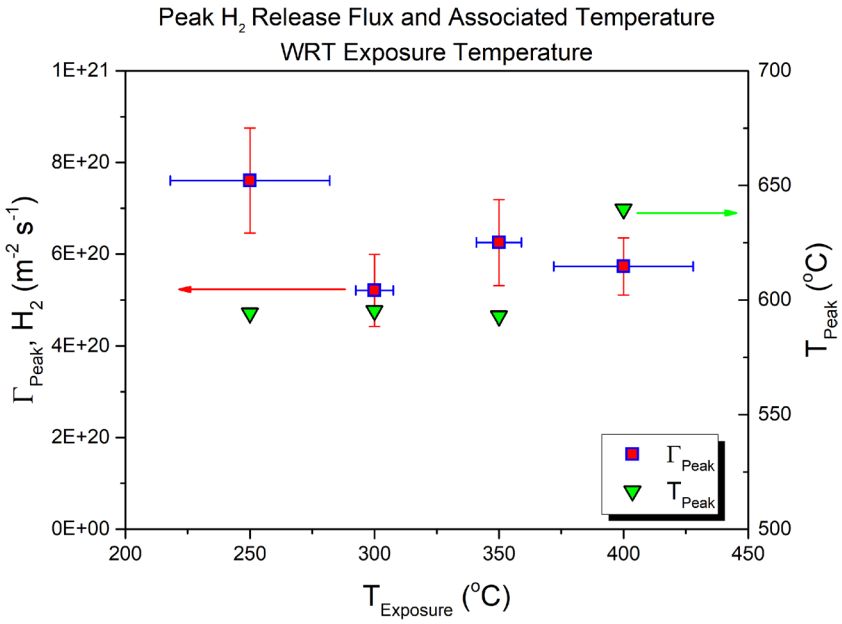

Figure 9. The peak release fluxes and the associated temperatures as a function of the sample temperature during exposure. Error associated with exposure temperature exists due to the additional heating from the plasma during exposure. Reproduced with permission from [24].

investigation is needed. This result, however is particularly important in informing the back-end processes that will be used to treat lithium streams exiting from reactors to recover and recycle deuterium and tritium fuel.

As a hydrogenated lithium sample is heated, not only does hydrogen begin to evolve from the α phase, as was claimed by Baldwin [10, 11], but LiH is also able to dissolve into solution to a greater degree. This enhanced, temperature-dependent dissolution of LiH complicates the simple time-integration used to evaluate the dissolved fraction for various exposure temperatures, and makes it appear as if more hydrogen had been absorbed into the α phase than actually had been. Proper evaluation of the true dissolved atomic fraction as a function of exposure temperature requires that one eliminate the contribution of the enhanced hydride dissolution to arrive at the actual amount of hydrogen that was originally absorbed in the α phase. Approximate models of the β contribution are needed because α phase hydrogen is lost during heating, causing fractions of LiH precipitate to dissolve before the plateau, in increasing amounts as temperature increases, in order to maintain thermodynamic equilibrium. All the while, more and more heat is lost to the LiH dissolution process until the plateau period is reached.

The contributions from β phase dissolution can be approximated, and can be subtracted from the total α phase evolution. Essentially, there exist two contributions to the evolution of hydrogen (assuming that the system is binary and consists only of Li and H—either in the α/dissolved or β/precipitated phase). Hydrogen is only able to readily evolve from the α phase, since in this phase hydrogen is less strongly bonded to the surrounding Li. Once in the plateau, the contributions to hydrogen evolution are almost entirely from the hydrogen

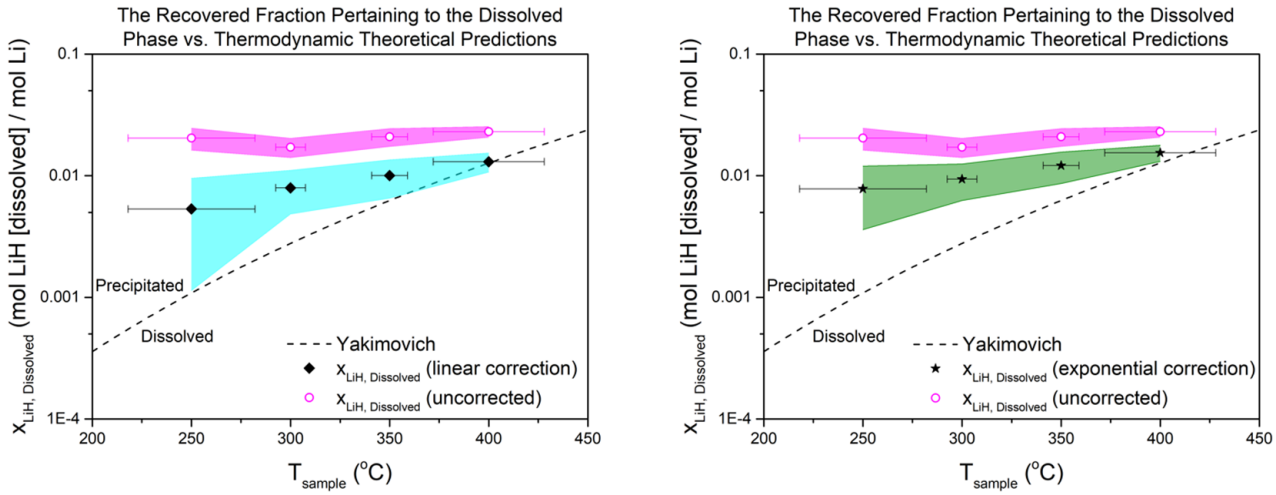

Figure 10. Plots illustrating the corrected dissolved fraction of LiH in Li solutions at various temperatures. These are plotted relative to the theory proposed by Yakimovich *et al* [26], which describes the thermodynamic solubility limitations. (Left) Black diamonds and the cyan shaded region represent the corrected data and error assuming a linear contribution from the β phase. (Right) Black stars and the olive shaded region represent the corrected data and error assuming an exponential contribution from the β phase. It should be noted that the points at 350 °C only include the data taken for the temperature dependence scan. This was done in order to prevent multivariate convolution. Reproduced with permission from [26].

in the β phase, which dissolves in order to maintain thermodynamic equilibrium with the α phase (which at this point is entirely sourced from the β phase). Prior to this plateau, however, α phase hydrogen is also being lost during heating. To compensate for this loss, small amounts of β phase hydrogen dissolves into solution, which then contribute to the overall hydrogen signal. To fully understand how each phase contributes to evolution rate/flux and how absorbed hydrogen was initially allocated to each of these phases, contributions from each must be deconvoluted from each other. A zeroth order approximation is to assume that β phase contributions increase linearly with heat (i.e. as α phase hydrogen is lost) from essentially negligible/zero to the plateau value. This linear contribution was then found, integrated, and subtracted from the total integrated hydrogen signal prior to the time at which the plateau desorption period was reached. The second 'correction' model in figure 10 is an exponentially increasing approximation with respect to heat input, which also manifests as an exponential with respect to time. This model was bounded in time similarly to how the previous linear model was bounded.

In figure 10, the corrected values are shown for the linear model on the left and the exponential model on the right. Associated error is shown in each plot, which is derived from the uncertainty propagation (using the variance formula) for the evolution rate based on the raw error associated with the hydrogen partial pressures measurements, the pressure calibration applied to these measurements, and the exposure temperatures. Uncertainty in evolution rate was then propagated once more, using a similar method, to arrive at the error bands displayed in figure 10, which are the standard deviations associated with each dissolved fraction.

Voltage appeared to have an effect on retention, as evidenced by the raw H_α OES scans, and desorption, as seen in the TPD trend scans. These effects seem to be related to the establishment of a thicker hydride surface saturation layer, a phenomenon which has also been observed for gaseous retention experiments [3, 4, 8, 9]. The fact that a more robust surface layer was formed is evidence that penetration depth, even at these relatively low energies, still affects the way hydrogen is retained by lithium. Release from the α phase subsequently requires more energy to disperse and break through the superficial surface layer. Changing the sample bias did not substantially affect the ratio of dissolved to precipitated hydride. There was a drop in this ratio for the sample biased to −100 V, however, the details of which will be left for future work. Penetration depth and bulk chemical interactions will need to be fully explored when determining what technologies can be used for tritium recovery.

The length of time the sample was exposed to a plasma appeared to have an interesting effect on the amount retained and subsequently released. For longer exposure times, diffusion of the insulating, surface hydride layer into the sample bulk is likely the mechanism by which a static sample undergoes volumetric conversion from lithium to lithium hydride in the presence of a hydrogen plasma. Future endeavors will seek to remedy this effect by employing a means to break down any insulating surface layer. This can be done either mechanically, or with surface treatment methods, such as electron beam irradiation. At the surface, the plasma acts to replenish the hydrogen transported into the bulk. Lithium flowing through a reactor will only be exposed to plasma for a short time, so the amount retained in a single pass will be quite low, with conversion to hydrides in the reactor only occurring after several passes through the vessel. Changing the exposure duration did not substantially affect the ratio of dissolved to precipitated hydride between the sample exposed for 15 min and the sample exposed for 60 min. There was a drop in this ratio for the sample exposed for 90 min, however. This may have been due to a number of factors, which will also be explored in more detail in the future.

In all cases, the recovered flux in the primary desorption period, considered to be recovery from the α phase, was found

to be quite low for the experimental temperatures and heating rates in this study. Recovery fluxes for H_2 were found to be, at maximum, nearly 8×10^{20} m^{-2} s^{-1}. To put these values in perspective, one can reference the in-vessel losses predicted by Krasheninnikov's work [27], which will be closer to 3×10^{21} T and D particles m^{-2} s^{-1} for a hypothetical liquid lithium-walled reactor. Isotopes absorbed during a single pass through the reactor will exit as the α phase. Treating these Li-rich streams using higher temperatures and heating rates may result in evolution fluxes that match these predicted losses; however, an argument must be made for efficiency. Large-scale, high-temperature heating of lithium volumetric rates on the order of 10's of liters per second will prove very difficult, even for systems that use inductive or laser heating. When isolating a Li-rich from a LiH-rich stream using upstream separation techniques, treating the latter will prove more effective for large-scale systems [28]. Having higher hydrogen populations will result in significantly enhanced recovery [29]. If these upstream separation techniques are absent, supplementary methods to improve isotope evolution in solutions with tritium populations below the solubility threshold will help to enhance recycling efficiency. Such supplementary methods will aid in enhancing recovery in thermal treatment modules, and have been described elsewhere [24], specifically with regards to ultrasonic degassing techniques, but require further investigation.

5. Conclusions

This work was focused on exposing liquid lithium samples to a variety of hydrogen plasma conditions, in order to investigate how ions and radicals alter the surface and sub-surface chemistry in hydrogen-lithium systems. The comprehension of these effects, and how they inform larger-scale systems, is crucial to the development of back-end technologies to recycle tritium from lithium in proposed lithium-walled fusion reactors. Two absorption periods were observed, which changed based on the exposure conditions. This was due to the thermodynamic and chemical responses at the surface and in the sample bulk. Similarly, the TPD scans taken for the liquid lithium samples showed two distinct desorption periods, which were reasoned to be due to the delineation between the α and β phases of hydrogen in lithium. This point was confirmed by the drastic changes in resistivity observed during TPD scans, which provided a novel condensed-phase analysis that was used to confirm conclusions from previous studies. At TUFCON-relevant energies, the effects plasmas have on dissolution enhancement appear to depend on sample exposure temperature. The additional kinetic energy from the plasma may be a more prominent contributor at lower sample temperatures, but this effect will require further investigation. The effects sample bias and exposure duration have on hydrogen absorption and desorption were also explored. The most important conclusions found in varying these parameters relate to the establishment of insulating surface layers and the mechanisms by which a static lithium sample undergoes volumetric conversion to a hydride.

Based on the results from this study, the release flux from lithium solutions with only α phase hydrogen (tritium, deuterium) are quite low for the experimental temperatures and heating rates. While fusion systems may be able to heat to higher temperatures at faster rates in order to remove hydrogen from this phase, isotope recovery efficiency would be dramatically improved by treating a hydride-rich stream separate from a lithium-rich stream. Future endeavors based on the results reported here should look to expand the scope to include a larger range of exposure variability, along with adding step-wise exposure monitoring. This will allow for a greater understanding of the kinetics and thermodynamics for these types of systems.

Acknowledgments

This work was supported by the Department of Energy, Fusion Energy Sciences: DOE/ALPS DEFG02-99ER54515.

References

[1] Mazzitelli G. *et al* 2010 Review of ftu results with the liquid lithium limiter *Fusion Eng. Des.* **85** 896–901 (*Proc. of the 1st Int. Workshop on Lithium Applications for the Boundary Control in Fusion Devices*)
[2] Majeski R. *et al* 2005 Recent liquid lithium limiter experiments in CDX-U *Nucl. Fusion* **45** 519
[3] Veleckis E., Deventer E.V. and Blander M. 1974 The lithium–lithium hydride system *J. Phys. Chem.* **78** 1933
[4] Veleckis E. 1977 Thermodynamics of the lithium–lithium deuteride system *J. Phys. Chem.* **81** 526
[5] Veleckis E., Yonco R. and Maroni V. 1977 Solubility of lithium deuteride in liquid lithium *J. Less-Common Met.* **55** 85
[6] Veleckis E. 1979 Decomposition pressures in the (+) fields of the Li–LiH, Li–LiD, and Li–LiT systems *J. Nucl. Mater.* **79** 20
[7] Adams P., Down M., Hubberstey P. and Pulham R. 1977 Solutions of lithium salts in liquid lithium: the electrical resistivity of solutions of nitride, hydride and deuteride *J. Chem. Soc. Faraday Trans.* **73** 230–5
[8] Hubberstey P., Pulham R.J. and Thunder A.E. 1976 Depression of the freezing point of lithium by nitrogen and by hydrogen *J. Chem. Soc. Faraday Trans.* **72** 431
[9] Katsuta H., Ishigai T. and Furukawa K. 1977 Equilibrium pressure and solubility of hydrogen in liquid lithium *Nucl. Technol.* **32** 7
[10] Baldwin M., Doerner R., Luckhardt S., Seraydarian R., Whyte D. and Conn R. 2002 Plasma interaction with liquid lithium: measurements of retention and erosion *Fusion Eng. Des.* **61–62** 231
[11] Baldwin M., Doerner R., Luckhardt S. and Conn R. 2002 Plasma interaction with liquid lithium: measurements of retention and erosion *Nucl. Fusion* **42** 1318
[12] Martin-Rojo A., Oyarzabal E., Morgan T. and Tabarés F. 2017 Exposure of liquid lithium confined in a capillary structure to high plasma fluxes in pilot-psi—influence of temperature on d retention *Fusion Eng. Des.* **117** 222–5
[13] Oyarzabal E., Martin-Rojo A. and Tabarés F. 2017 Laboratory experiments of uptake and release of hydrogen isotopes in liquid lithium *J. Nucl. Mater.* **463** 1173–6
[14] Mundra K. and Debroy T. 1995 A general model for partitioning of gases between a metal and its plasma environment *Metall. Mater. Trans.* **26B** 149

[15] Ohno S. and Uda M. 1980 Vacuum-extraction method for hydrogen determination in weld metals: an analysis of hydrogen behavior in the JIS type weld specimen *J. Japan Weld. Soc.* **49** 747–54

[16] Ohno S. and Uda M. 1981 Effects of hydrogen and nitrogen on blowhole formation in pure nickel at arc welding and non-arc melting *Trans. Natl Res. Inst. Met.* **23** 243–8

[17] Katz J. and King T. 1989 Kinetics of nitrogen absorption and desorption from a plasma arc by molten iron *Metall. Trans.* **20B** 175

[18] Bandopadhyay A., Banerjee A. and Debroy T. 1992 Nitrogen activity determination in plasmas *Metall. Trans.* B **23** 207–14

[19] Gedeon S.A., Sorensen C.D., Ulrich K.T. and Eagar T. 1987 Measurement of dynamic electrical and mechanical properties of resistance spot welds *WRC Bull.* **322** 378–85

[20] Pehlke R. 1979 *Unit Processes in Extractive Metallurgy* 4th edn (New York: Elsevier)

[21] Fiflis P., Curreli D. and Ruzic D. 2015 Direct time-resolved observation of tungsten nanostructured growth due to helium plasma exposure *Nucl. Fusion* **55** 033020

[22] Tobe R., Sekiguchi A., Sasaki M., Okada O. and Hosokawa N. 1996 Plasma-enhanced CVD of TiN and Ti using low-pressure and high-density helicon plasma *Thin Solid Films* **155** 281–2

[23] Sudit I. and Chen F. 1994 RF compensated probes for high-density discharges *Plasma Sources Sci. Technol.* **3** 162

[24] Christenson M.P. 2018 The design and development of hydrogen isotope extraction technologies for a limit-style liquid lithium loop *PhD Thesis* University of Illinois at Urbana-Champaign

[25] Smith R. and Miser J. 1963 *Compilation of the Properties of Lithium Hydride* (Cleveland OH: NASA Technical Memorandum) p x-483

[26] Yakimovich K. and Biryukova T. 2012 Thermodynamic properties of Li–LiH (LiD, LiT) systems. the phase diagram *Open J. Phys. Chem.* **2** 141

[27] Krasheninnikov S., Zakharov L. and Pereverzev G. 2003 On lithium walls and the performance of magnetic fusion devices *Phys. Plasmas* **10** 1678

[28] Ono M., Majeski R., Jaworski M., Hirooka Y., Kaita R., Gray T., Maingi R., Skinner C., Christenson M. and Ruzic D. 2017 Liquid lithium loop system to solve challenging technology issues for fusion power plant *Nucl. Fusion* **57** 116056

[29] Christenson M., Moynihan C. and Ruzic D. 2018 A distillation column for hydrogen isotope removal from liquid lithium *Fusion Eng. Des.* **135** 81–7